Advanced Powder Technology

Research on Microwave Drying Technology in the Procedure of Preparation of V2O5 from Ammonium Polyvanadate (APV)

--Manuscript Draft--

Manuscript Number:	ADVPT-D-20-00814R2
Article Type:	Original Research Paper
Keywords:	microwave heating; ammonium polyvanadate (APV); vanadium pentoxide; factors optimization; dynamic mechanism
Corresponding Author:	Lei Gao, Ph.D Yunnan Minzu University Kunming, CHINA
First Author:	Hewen Zheng
Order of Authors:	Hewen Zheng
	Qiannan Li
	Yeqing Ling
	Mamdouh Omran
	Lei Gao, Ph.D
	Jin Chen
	Guo Chen
Abstract:	High-quality vanadium pentoxide powder is an important product of the vanadium industry and was usually prepared from ammonium polyvanadate (APV) using a roasting process combined with a drying pretreatment. Conventional hot air drying is usually used for the drying of APV, the heat transfer of which is from outside to inside thus limited the efficiency of the drying pretreatment. In the present paper, microwave heating was applied as an alternative heating method for the drying of APV because of its advantages including selective heating, high heating efficiency, low energy consumption, and green environmental protection. An experimental comparison between hot air drying and microwave drying is provided, and the results show that microwave drying is more energy-saving and faster. The drying characteristics of APV under the irradiation of microwave energy were investigated. The influences of factors including microwave power, material quality, and initial moisture content on microwave drying were studied. The results show that the microwave power, initial moisture content, and initial mass are positively proportional to the microwave drying efficiency of APV. Additionally, the Page model was robust in describing the kinetics of microwave drying and hot air drying of APV. This study provides fundamental knowledge on the microwave drying process and provides the trial for the industrial applications of microwave heating on the preparation of V_2O_5.

Research on Microwave Drying Technology in the Procedure of Preparation of V_2O_5 from Ammonium Polyvanadate (APV)

Hewen Zheng [a, b], Qiannan Li [a, b], Yeqing Ling [a, b], Mamdouh Omran [c], Lei Gao [a, *], Jin Chen [b, **], Guo Chen [a, b, **]

[a] *Kunming Key Laboratory of Energy Materials Chemistry, Key Laboratory of Green-Chemistry Materials in University of Yunnan Province, Yunnan Minzu University, Kunming 650500, PR China.*

[b] *Key Laboratory of Unconventional Metallurgy, Ministry of Education, Kunming University of Science and Technology, Kunming 650500, PR China.*

[c] *Faculty of Technology, University of Oulu, Finland.*

[*] Corresponding author: leigao@ymu.edu.cn. Tel: +86-871-65910017; Fax: +86-871-65910017.

[**] Co-corresponding author: jinchen@kust.edu.cn, guochen@kust.edu.cn

Abstract

High-quality vanadium pentoxide powder is an important product of the vanadium industry and was usually prepared from ammonium polyvanadate (APV) using a roasting process combined with a drying pretreatment. Conventional hot air drying is usually used for the drying of APV, the heat transfer of which is from outside to inside thus limited the efficiency of the drying pretreatment. In the present paper, microwave heating was applied as an alternative heating method for the drying of APV because of its advantages including selective heating, high heating efficiency, low energy consumption, and green environmental protection. An experimental comparison between hot air drying and microwave drying is provided, and the results show that microwave drying is more energy-saving and faster. The drying characteristics of APV under the irradiation of microwave energy were investigated. The influences of factors including microwave power, material quality, and initial moisture content on microwave drying were studied. The results show that the microwave power, initial moisture content, and initial mass are positively proportional to the microwave drying efficiency of APV. Additionally, the Page model was robust in describing the kinetics of microwave drying and hot air drying of APV. This study provides fundamental knowledge on the microwave drying process and provides the trial for the industrial applications of microwave heating on the preparation of V_2O_5.

Keywords: microwave heating; ammonium polyvanadate (APV); vanadium pentoxide; factors optimisation; dynamic mechanism

1 Introduction

Vanadium pentoxide (V_2O_5) is an acidic crystalline powder widely used in metallurgy, chemical industry, steel, etc., and is also a fundamental product of the vanadium industry. V_2O_5 powder is an important basic raw material for preparating vanadium aluminium alloy, an important fundamental material with decent cold working performance, heat resistance, welding performance, and mechanical strength [1,2]. V_2O_5 also has applications as an electrode material and is a fundamental material for vanadium lithium battery and all vanadium liquid flow batteries [3-8]. As an anode material for lithium-ion batteries, V_2O_5 has the advantages of large specific capacity, high voltage, and low price [9]. For the application of V_2O_5 in all vanadium liquid flow batteries, V_2O_5 is an important alternative material for $VOSO_4$ to reduce the cost of the products [10,11].

Recently, the growing requirement for the continuous supplement of high-quality V_2O_5 powder appears because of the fast development of the military, aerospace industry, and other fields. High purity V_2O_5 powder was synthesised from an intermediate product, namely APV, which is prepared from vanadium-containing solutions, and manipulated into various microstructure forms including nest-like structure, nanosheets, etc [12,13]. For the potential industrial application of these high-performance V_2O_5 powder, attentions have been paid on the pretreatment technology of APV. It is noticed that APV contains a large amount of water content which increases risks of combustion caused by the volume expansion during the transformation of water into vapour at high temperature. Thus, for the roasting of

APV, the drying process is required as an important pretreatment process [14].

Among the drying technologies of APV, conventional hot air drying is usually used whilst it has disadvantages including low efficiency, energy-consuming, and inhomogeneous temperature gradient. Thus, the development of an alternative drying technology to provide solutions for the above issues is in urgent demand. As a novel drying technology, microwave drying is firstly noticed in food industries to provide fast drying and elaborate quality control of the final products, and is spreading in more fields including chemical process, metallurgy, and materials manipulation [15]. Microwave is a kind of electromagnetic wave with strong penetrating since it has a frequency between 0.3 and 300 GHz with corresponding wavelengths ranging from 1 m to 1 mm. The interaction between polar molecules in the material and microwave electromagnetic field makes the microwave energy convert into heat energy to heat materials on a macro level [16-20], and thus microwave heating technology shows many advantages including fast drying rate, high product quality [21-25]; high efficiency and energy saving [26]; selective heating [27-29]; green cleaning [30-34], etc. Li et al. [35] prepared CaO-doped partially stabilised zircona (CaO-PSZ) with fused zirconia as raw material by microwave heating technology and determined the stable parameters for the preparation of CaO-PSZ. Thus, the application of microwave drying technology on the pretreatment shows a good prospect for a further improvement on the heating rates and the quality of drying products [36,37].

The advantages of microwave heating are resulting from its unique heating mechanism. For the application of microwave drying process, the advantages can be

explained with the contrast between the heat and mass transfer models of microwave drying and conventional heating as shown in Fig. 1: the heat transfer direction of conventional drying is from outside of the material to the inside of the material, and the temperature gradient provides less assistance on the mass transfer of moisture from the inside to the outside [38]. Thus, in some cases, mass transfer of moisture inside the material became a controlling step of the whole drying process, and the only optimising method is to further increase the drying temperature accompanying with high energy consumption [39].

Under the radiation of microwave, the moisture inside the material will preferentially absorb the microwave energy which subsequently converts into energy for heating. Since the microwave can penetrate the material, the temperature gradient caused by the microwave heating is slight, and the moisture inside the material continuously diffuses from the inside to the surface for evapouration. Since the temperature gradient, heat transfer, and vapour pressure transfer direction inside the material provides few resistances on the water transfer direction, the diffusion process is encouraged, the cost for energy can be reduced and the dry efficiency can be largely improved [40].

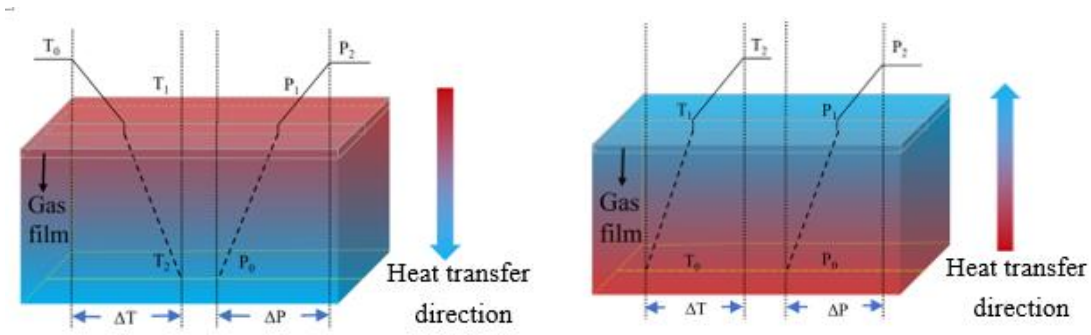

(a) (b)

Fig. 1. Heat and mass transfer models during (a) conventional drying; (b) microwave drying [38].

At present, many studies on the application of microwave drying for minerals including lignite, pyrolusite, tungsten concentrate were reported, and the corresponding kinetics were studied [41-45]. Xu et al. [44] analysed the drying kinetics of lignite by using the Dolye temperature integral model and Coats-Redfern integral model, indicating that the drying kinetics equation of lignite in the non-isothermal drying process can be described by the Dolye model. Li et al. [24] studied the drying kinetics of microwave drying for ilmenite under the condition that the mass of ilmenite was 25g and the microwave power was 385W, indicating that Page's semi-empirical model was better than the Henderson-Pabis index model for the description of the process. Du et al. [46] studied the microwave drying characteristics and dynamic model of pyrolusite, the results showed that with the increase of the particle size and microwave power of pyrolusite, the microwave drying rate increased, and the drying efficiency increased; and the diffusion approach model was more consistent with the description of the microwave drying process of pyrolusite. Tahmasebi et al. [47] investigated the drying kinetics of Chinese lignite in nitrogen fluidised-bed, superheated steam fluidised-bed, and the radiation of microwave energy, ten different thin-layer empirical drying models were employed for the fitting of time-dependent moisture ratios. The results indicated that the Midilli-Kucuk model was most suitable for describing the nitrogen fluidised-bed process and superheated steam fluidised-bed

process, whilst the Page model was most suitable for describing the microwave drying process. However, there are relatively few studies on the application of microwave drying on APV and the corresponding kinetics.

In this paper, the microwave drying pretreatment of APV for the preparation of V_2O_5 powder was studied, and the effects of microwave power, mass, and initial moisture content on the products were declared. Simultaneously, conventional drying and microwave drying were compared to checking the advantages of microwave drying. To understand the fundamental of microwave drying and conventional drying process of APV, four classical kinetic models, namely Page model, Verma model, Simplified Fick's dispersion model, and Two-term experimental model were employed for experimental data fitting. The aim was to provide fundamental research data for the development of industrial drying technology.

2. Experimental section

The experimental equipment for microwave drying of APV is shown in Fig. 2, which mainly consists of the following parts: a microwave oven, an induction heater, a cooling water system, a temperature detection system, and a computer system. Besides, the electronic balance (AL-104) was placed above the microwave oven and connected with the internal quartz balance to read the time-dependent data of material quality. The maximum power of the microwave oven was 700W, and the frequency was 2.45GHz with a working voltage of 220V. The details for the using powers and its pulse interval heating durations are shown in Table 1.

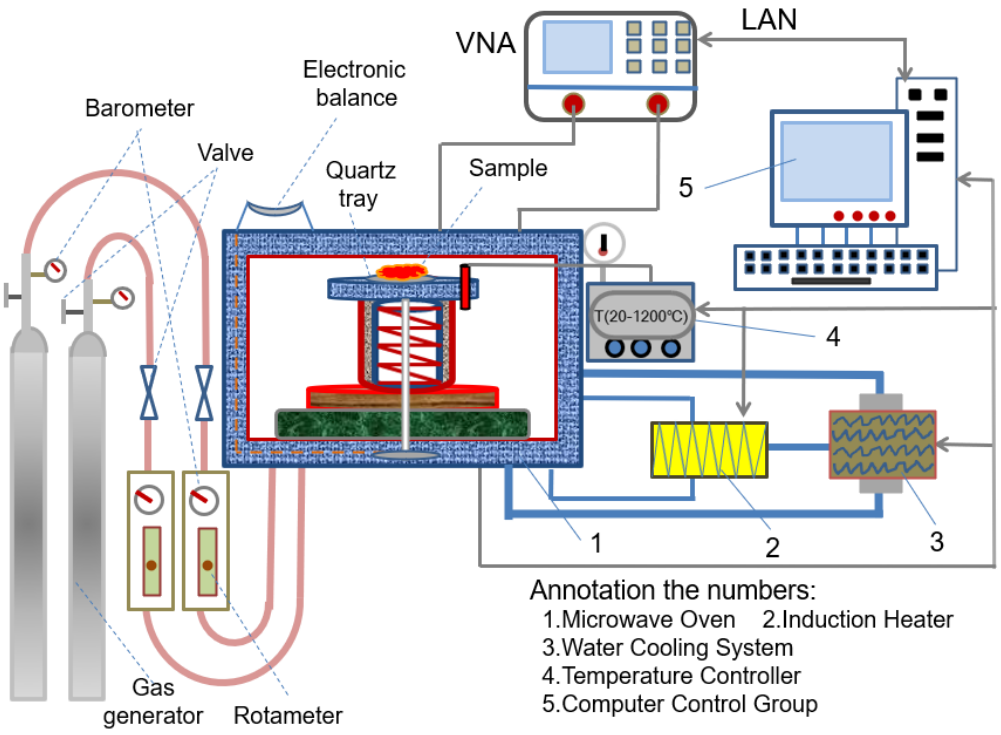

Fig. 2. The schematic diagram of equipment for microwave drying of APV.

Table 1 Microwave working/stopping time and microwave power converted at different positions.

	100%	80%	50%	40%
Working / Stopping time (S)	30/0	24/6	15/15	12/18
Converted power (W)	700	560	350	280

2.1 Chemicals and Materials

In this experiment, APV was sourced from Hubei Xinrunde Chemical Limited Company, Wuhan City, Hubei Province. The chemical compositions of the as-received APV are shown in Table 2, revealing 64.55% of V, 26.99% of O, 8.00% of N, and a small number of other elements including Fe, S, Na, K, and Si.

Table 2 Main chemical composition of the APV.

Composition	V	O	N	Fe	S	Na	K	Si
Mass%	64.55	26.99	8.00	0.097	0.092	0.052	0.046	0.054

A particle size analyser (Mastersiser-3000) was used to analyse the sieved APV powder within a measurement range of 10nm to 3.5mm. The particle size distribution histograms and the corresponding cumulative volume distribution curve are shown in Fig. 2. The related characteristic analysis on the particle size distribution of the as-received APV is shown in Table 3, revealing that the particle size distribution range of APV was 3.28-29.24 μm, volume mean diameter of the as-received APV powder was 10.04 μm, and median particle size D50 of the as-received APV powder was 7.24 μm.

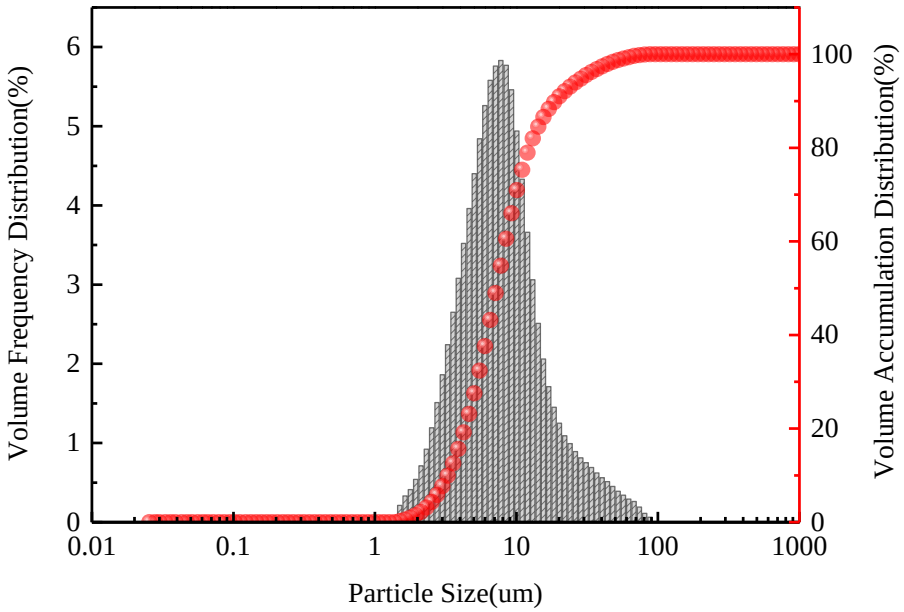

Fig. 3. Particle size distribution histograms and the corresponding cumulative volume distribution curve.

Table 3 Characteristic analysis on the particle size distribution of the as-received

APV.

Particle size distribution ratio	D_{10}	D_{20}	D_{30}	D_{40}	D_{50}	D_{60}	D_{70}	D_{80}	D_{90}	D_{95}	Mz
Particle size /μm	3.28	4.32	5.28	6.22	7.24	8.41	9.92	12.34	18.82	29.24	10.04

2.2 Microwave drying experimental procedure

To understand the influences of microwave power, the weight of the material, and initial moisture content on the drying efficiency of APV, drying experimental procedures were designed in the present study.

(1) Microwave power

To explore the influence of microwave power on the drying characteristics of APV, four groups of as-received APV with a mass of 20g and an initial moisture content of 20% were selected, and heated in the microwave oven with a microwave power of 280W, 350W, 560W, and 700W, respectively. During the experiments, the corresponding sample mass was read and recorded every 30 seconds.

(2) Weight of the material

To explore the influence of the weight of the material on the drying characteristics of APV, three groups of as-received APV with a microwave power of 560W and an initial moisture content of 20% were selected, and heated in the microwave oven with a microwave power of 10.00g, 20.00g, and 30.00g, respectively.

During the experiments, the corresponding sample mass was read and recorded every 30 seconds.

(3) Initial moisture content

To explore the influence of initial moisture content on the drying characteristics of APV, three groups of as-received APV with a microwave power of 560W and a mass of 20g were selected, and heated in the microwave oven with an initial moisture content of 10%, 20%, and 35%, respectively. During the experiments, the corresponding sample mass was read and recorded every 30 seconds.

2.3 Experimental procedure of hot air drying

To discuss the difference between hot air drying and microwave drying, an experimental program of hot air drying was designed. APV with a mass of 20g and initial water content of 20% was put into a blast drying oven for conventional drying. The temperature in the blast drying oven was 300 ° C, and the mass of APV was measured in a cycle of 30s.

2.4 Residual moisture analysis

According to the mass conservation law of APV (APV), the residual moisture M_t after drying for time t can be calculated with the following equation under ideal conditions:

$$M_t = (m_t - m_{dt})/m_{dt} \times 100\% \quad (1)$$

where m_t represents the mass of APV after drying for time *t*, and m_{dt} is the dry basis mass of APV. Subsequently, the drying rate (DR) can be defined as the change in moisture content per unit time (t) as follows:

$$\mathrm{DR} = \mathrm{d}Mt/\mathrm{d}t \tag{2}$$

2.5 Drying kinetic model

The study of drying kinetics is based on the mathematical simulation of the thin-layer drying curve. There are many mathematical equations of the thin layer drying, which are divided into the theoretical equation, semi theoretical equation, semi-empirical equation, and empirical equation. The semi-empirical equation is widely used because of its high accuracy and wide application range. In 1949, Page modified the Lewis model and got Page model, which was widely used in grain drying experiments [48,49]. In 1980, Sharaf eldeen et al. obtained a Two-term exponentials model based on Henderson and Pabis model [50]. In 1985, Verma et al. obtained the Verma model through rice drying experiment and numerical simulation with Henderson and Pabis model [51]. According to the Page model, the Simplified Fick's diffusion model is derived from Fick's second law [52].

To understand the kinetics of the microwave drying process of APV, four classical kinetic models, namely Page model, Verma model, Simplified Fick's dispersion model, and Two-term experimental model were employed for data fitting of experimental results as shown in Table 4. The aim was to provide fundamental research data for the development of industrial drying technology.

Table 4 Drying kinetic models used for data fitting.

	Model	Model equation
1	Page [48,49]	$MR = exp(-kt^n)$
2	Two-term exponentials [50]	$MR = aexp(-kt) + (1-a)exp(-kat)$
3	Verma [51]	$MR = aexp(-kt) + (1-a)exp(-gt)$
4	Simplified Fick's diffusion [52]	$MR = aexp(-ct/L^2)$

In Table 4, *MR* is the effective water ratio, $M_R = (M_t - M_e)/(M_0 - M_e)$, %, where M_e is the equilibrium moisture content and M_0 is the initial moisture content; t is the time; a, c, g is the empirical coefficient in the drying model; k is the drying constant, s^{-1}; n is the undetermined coefficient related to the drying conditions; L is the plate thickness, m.

The corresponding fitting curves can provide the relevance between the experimental data and the kinetics model, the standards for estimating the relevance including correlation coefficient R^2, residual square sum (RSS), and F-Value.

3. Results and discussion

3.1 Effect of microwave power on microwave drying of APV

The time-dependent curves of moisture content of APV and the corresponding drying rates are shown in Fig. 4, resulting from different microwave powers of 280W,

350W, 560W, and 700W, with an initial mass of 20g and an initial moisture content of 20%.

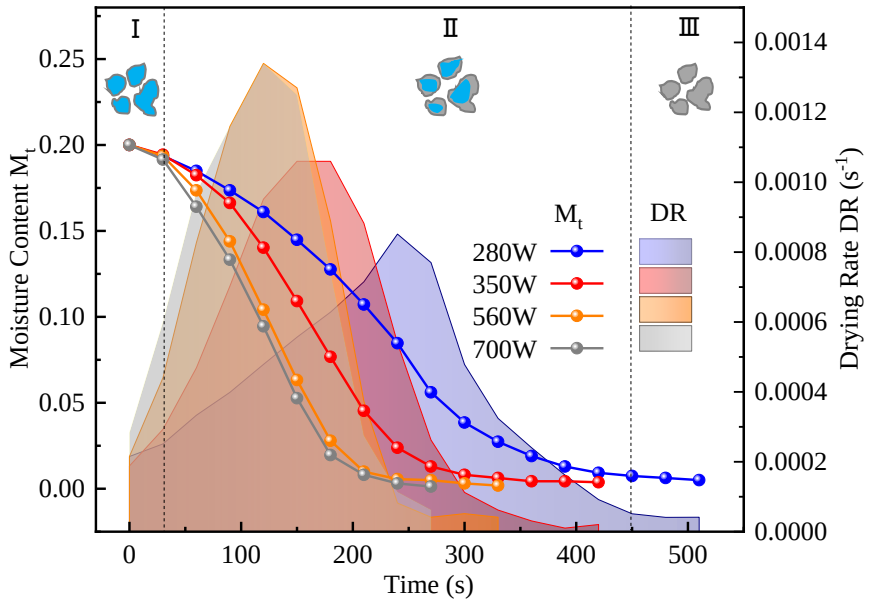

Fig. 4. Curves of weight loss and drying rates of APV with different microwave power and an initial sample mass of 20g, 20% of moisture content.

The moisture content curves indicated that the drying process of APV can be divided into three stages. The schematic diagram for stage I, stage II, and stage III are shown in Fig. 4 with the corresponding moisture content under microwave power of 280W. At stage I with a time duration of 0-30s, the absorbed microwave energy was the heat source for preheating of free moisture and the energy source for the absorption latent heat before vapourisation, thus few changes were found on the moisture content of the as-received APV. At stage II with a time duration of 30-450s, the evapouration process occurred, the moisture content continuously transferred from inside of the as-received sample to the surface boundary to evapourate into the environment. Stage III with a time duration of 450-510s was the end of the evapouration process, the changes on the moisture content curve turned to be gentle,

rendering to a slight drying efficiency and low profits for the further extension of the drying process. Clearly, with the increase of microwave power for the drying process, a slight change was found for the duration of stage I in the studied range, whilst a significant reduction was noticed for the duration of stage II.

To quantitatively understand the effect of microwave power on the drying efficiency, the drying rates DR were calculated based on the slopes of the curves of moisture content M_t, rendering to the maximum drying rate of APV with microwave powers of 280W, 350W, 560W, and 700W were $0.000852s^{-1}$, $0.00106s^{-1}$, $0.00134s^{-1}$ and $0.00134s^{-1}$, respectively. The corresponding time for reaching these peak drying rates were 240s, 150s, 120s, and 120s, respectively. The corresponding average drying rates were $0.000368s^{-1}$, $0.000443s^{-1}$, $0.000561s^{-1}$ and $0.000680s^{-1}$, respectively.

The noticed trend for the variation of DR can be explained with the following hypothesis: the microwave absorption performance of material has positive relations with its complex dielectric constant ε^* and loss tangent coefficient $\tan\delta$. Since water has decent values of ε^* and $\tan\delta$, the loss of water during the drying process may cause the decrease of microwave absorption performance of the mixture, resulting in a decrease in the temperature increasing rate. Thus, DR has shown a peak value in the time duration around 100s-200s, resulting from the temperature increasing rate affected by the procedure of drying process in the studied range.

The drying performance of the as-received powder at a microwave power of 560W was better than that at microwave powers of 280W and 350W and was close to that at a microwave power of 700W. Thus, 560W is a decent choice of microwave

power for the subsequent experimental study from the viewpoint of saving energy.

3.2 Effect of quality on microwave drying of APV

The time-dependent curves of moisture content of APV and the corresponding drying rates are shown in Fig. 5, resulting from different initial sample masses of 10g, 20g, and 30g, with a microwave power of 560W and an initial moisture content of 20%.

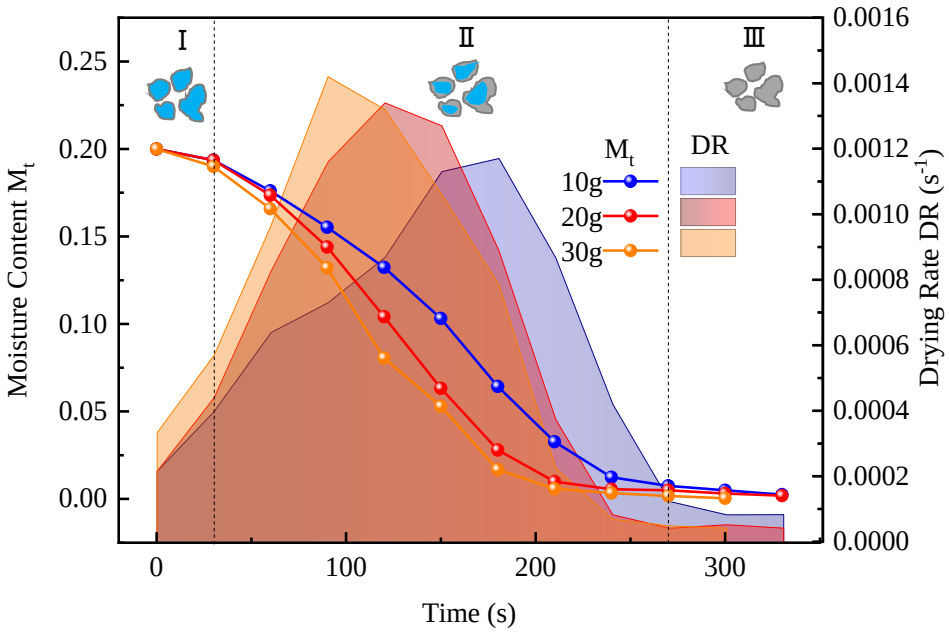

Fig. 5. Curves of weight loss and drying rates of APV with different sample mass and a microwave power of 560W, 20% of moisture content.

The results indicated that the mass of the as-received sample has a slight influence on the division durations of the stages. The duration for stage I all ended at the 30s, and the duration for stage II all ended at 270s. For the mass of APV powder of 10g, 20g, and 30g at a heating time of 330s, the dehydration rates were 99.00%, 99.25%, and 99.83% respectively. The final moisture contents were 1.25%, 0.94%

and 0.21%, respectively.

To quantitatively understand the effect of sample mass on the drying efficiency, the drying rates DR were calculated based on the slopes of the curves of moisture content M_t, rendering to the maximum drying rate of APV with sample masses of 10g, 20g, and 30g were $0.00117s^{-1}$, $0.00134s^{-1}$, and $0.00142s^{-1}$, respectively. The corresponding time for reaching these peak drying rates were 180s, 120s, and 90s, respectively. The corresponding average drying rates were $0.000560s^{-1}$, $0.000561s^{-1}$ and $0.000622s^{-1}$, respectively. The drying performance of the as-received sample at a sample mass of 30g was better than that at a sample mass of 10g or 20g, which was contrary to the common sense received from conventional heating. It should be noticed that this conclusion only fits in the studied sample quality range. For samples with large quantities, the heating efficiency may show a negative relation with sample mass depending on the penetrate thickness of the microwave on the sample, which needs further investigation.

3.3 Effect of initial moisture content on microwave drying of APV

The time-dependent curves of moisture content of APV powder and the corresponding drying rates are shown in Fig. 6, resulting from the different initial moisture content of 10%, 20%, and 30%, with a microwave power of 560W and a sample mass content of 20g.

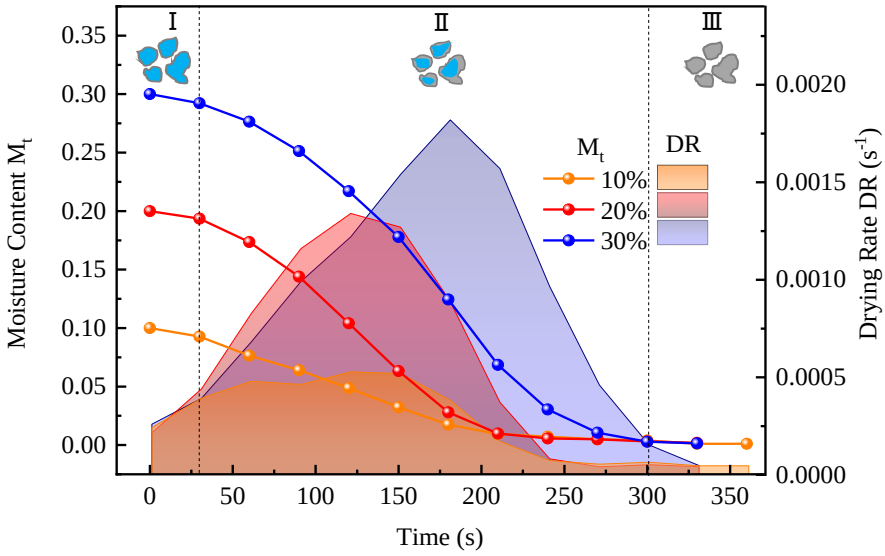

Fig. 6. Curves of weight loss and drying rates of APV with different initial moisture content and a microwave power of 560W, 20g of sample mass.

The results indicated that the initial moisture content of the as-received sample influences the division durations of the stages. The durations for stage I was in a range of 0-30s, whilst the duration of stage Ⅱ was extended with the increase of moisture content. For M_t value of 10% and 20%, stage Ⅱ ended at 210s, whilst for M_t value of 30%, stage Ⅱ ended at 300s. For the initial moisture contents of APV with 10%, 20%, and 30% at a heating time of 360s, the dehydration rates were 98.9%, 99.3%, and 99.7% respectively. The final moisture contents were 1.10%, 0.94% and 0.48%, respectively. To quantitatively understand the effect of initial moisture content on the drying efficiency, the drying rates DR were calculated based on the slopes of the curves of moisture content Mt, rendering to the maximum drying rate of APV with initial moisture contents of 10%, 20%, and 30% were 0.000382s^{-1}, 0.00134s^{-1}, and 0.00182s^{-1}, respectively. The corresponding time for reaching these peak drying rates were 120s, 120s, and 180s, respectively. The corresponding average drying rates were

0.000266s^{-1}, 0.000561s^{-1} and 0.000842s^{-1}, respectively. The drying performance of the as-received sample at an initial moisture content of 30% was better than that at an initial moisture content of 10% or 20%, which was benefiting from the positive relation between moisture content and microwave energy absorption efficiency, and was contrary to the common sense received from conventional heating.

3.4 Experimental results and comparison of hot air drying

The experimental data of hot air drying at 300 °C is close to the experimental data of microwave drying with a microwave power of 560W. Therefore, two groups of experimental data are selected for comparison, as shown in Fig. 7.

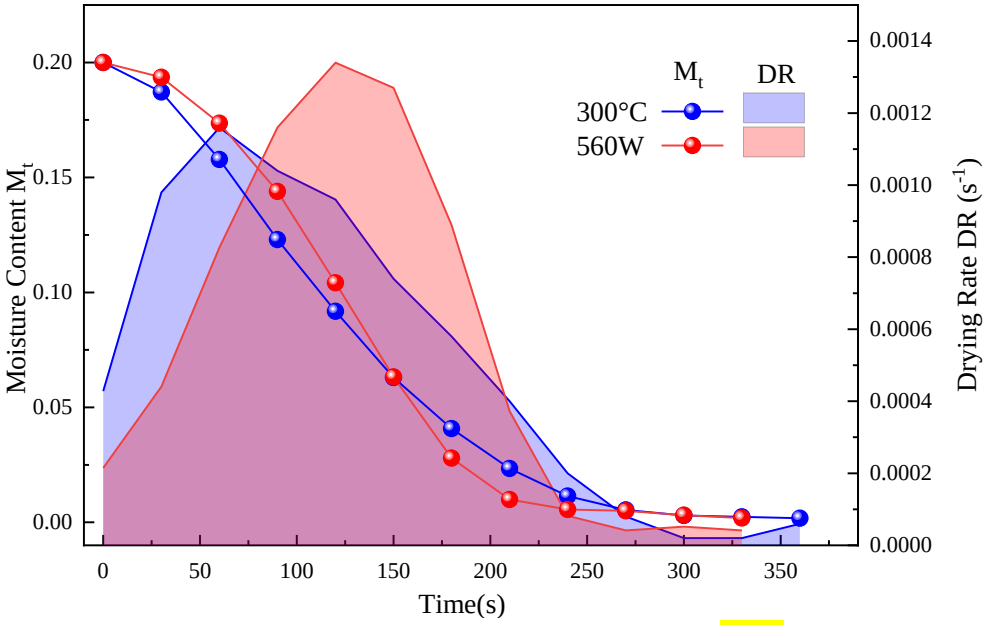

Fig. 7. Curves of moisture content and drying rate of APV under microwave drying and hot air drying.

According to the data, it can be known that the maximum drying rate of hot air drying is 0.00116s^{-1} in the 60s, the whole drying process lasts 360s, and the average drying rate is 0.000551s^{-1}. Compared with microwave drying which has a surface

temperature range of 180-190 °C, the hot air drying is more energy-consumption and slower.

3.5 Drying kinetic model fitting

3.5.1 Kinetic analysis of microwave drying

To understand the kinetics during microwave drying, four kinetic models in Table 4, namely Page model, Verma model, Simplified Fick's dispersion model, and Two-term experimental model were employed for experimental data fitting resulting from the water content curve of APV under different microwave power. As a result, the fitting curves are shown in Fig. 8, and the corresponding fitting coefficient (R^2), residual square sum (RSS), F-Value, and other parameters are presented in Table 5. The fitting results in Table 5 indicated that the corresponding average values of R^2 were 0.997928, 0.936243, 0.889073, and 0.973543, respectively. The corresponding average values of RSS were 0.003858, 0.105688, 0.177938 and 0.047298, respectively. the corresponding average values of F-Value were 7439.828, 141.9349, 83.91454, and 527.3807, respectively.

The above-average value indicated that the Page model was most suitable for describing the drying kinetics of APV powder in the studied microwave power range since the RSS value of the Page model was smallest and the corresponding R^2 value and F-Value were largest among those resulting from the selected models.

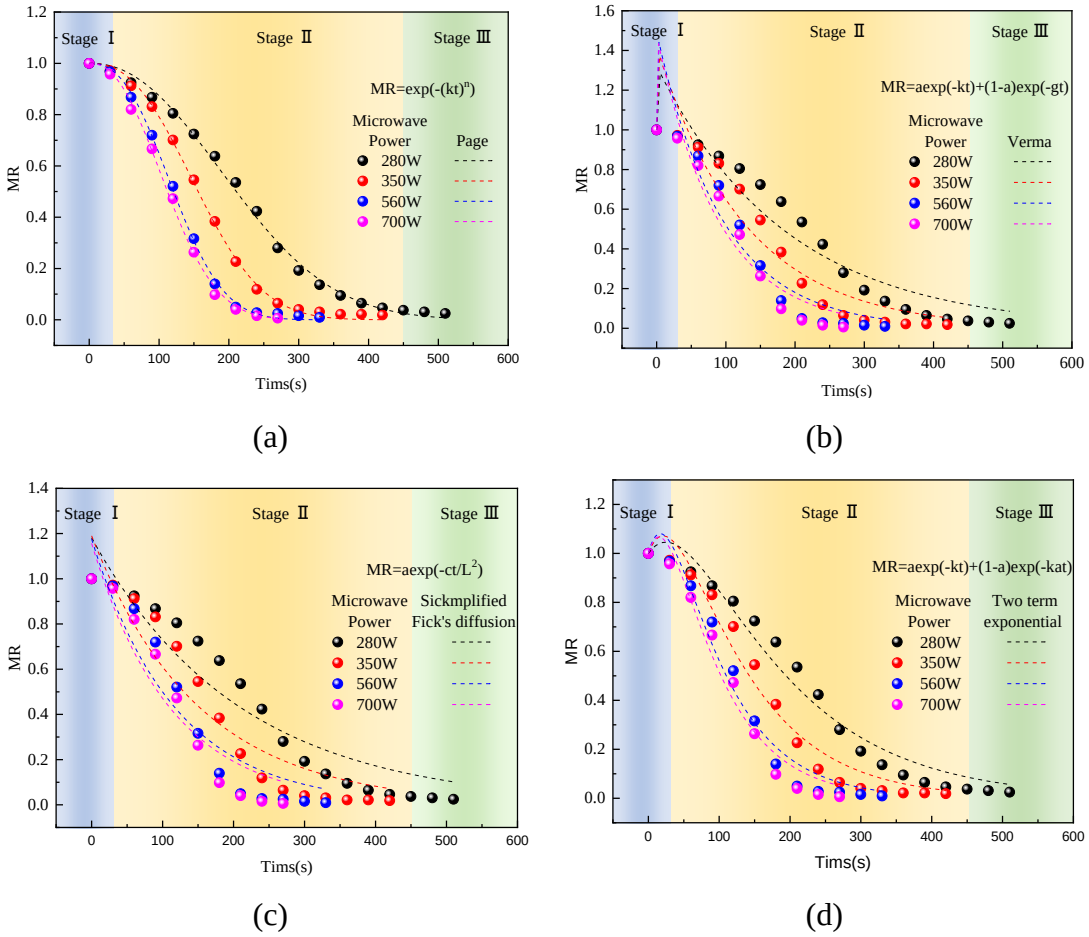

Fig. 8. Fitting curves of experimental data under different drying kinetic models and different microwave power resulting from: (a) Page; (b) Verma; (c) Simplified Fick's dispersion; (d) Two-term experimental.

Table 5 Fitting results of drying kinetics with experimental data.

Model	Microwave Power/W	Params	R^2	RSS	F-value
Page	280W	k=5.4019*10^{-6} , n=2.19841	0.99655	0.0077	5961.64
	350W	k=2.9680*10^{-6} , n=2.44772	0.99849	0.00303	9606.47
	560W	k=4.9419*10^{-6} , n=2.47144	0.99883	0.00191	9412.29
	700W	k=1.3449*10^{-5} , n=2.29901	0.99784	0.00279	4778.91
	280W	k=0.00535 , a=1.32185 g=24642.81668	0.92903	0.14822	188.71724

Verma	350W	k=0.00781，a=1.41793 g=25821.68216	0.93557	0.11957	145.7932
	560W	k=0.01056，a=1.49248 g=24642.81668	0.94156	0.08575	123.02713
	700W	k=0.01122，a=1.47765 g=21916.71758	0.93881	0.06921	110.20183
Simplified Fick's diffusion	280W	a=1.18137，c=0.0194 L=2.00843	0.90141	0.2059	134.45064
	350W	a=1.19008，c=0.02601 L=1.97403	0.89385	0.19697	86.92662
	560W	a=1.17594，c=0.03421 L=1.9986	0.88518	0.16847	61.1454
	700W	a=1.15692，c=0.03749 L=2.04282	0.87585	0.14041	53.13551
Two term exponential	280W	k=0.00722，a=2.25102	0.97294	0.06029	754.02274
	350W	k=0.01017，a=2.32533	0.97427	0.05172	556.25695
	560W	k=0.0133，a=2.34996	0.97446	0.04164	427.58464
	700W	k=0.01408，a=2.31411	0.9725	0.03554	371.65853

To avoid the occasionality for the results received from data fitting in Table 5, the experimental data resulting from changes in the quality of the as-received sample and changes in the initial moisture content were also used for data fitting. The corresponding fitting curves are shown in Fig. 9 and Fig. 10, respectively, and the corresponding fitting coefficient (R^2), residual square sum (RSS), F-Value, and other parameters are presented in Table 6 and Table 8, respectively. The fitting results in Table 6 indicating that the corresponding average values of R^2 were 0.99746, 0.93604, 0.91669, and 0.88137, respectively. The corresponding average values of RSS were

0.003913, 0.088957, 0.114137 and 0.18374, respectively. The corresponding average values of F-Value were 5848.898, 118.4166, 96.13579, and 298.0208, respectively. The fitting results in Table 7 indicating that the corresponding average values of R^2 were 0.997453, 0.93542, 0.88839, and 0.971137, respectively. The corresponding average values of RSS were 0.003983, 0.09288, 0.16027 and 0.046147, respectively. The corresponding average values of F-Value were 5862.285, 169.4419, 84.4079, and 651.1681, respectively.

The data in the tables further confirming that the fitting degree of the Page model was relatively decent, and the Page model was most suitable for describing the microwave drying process of APV among the selected models.

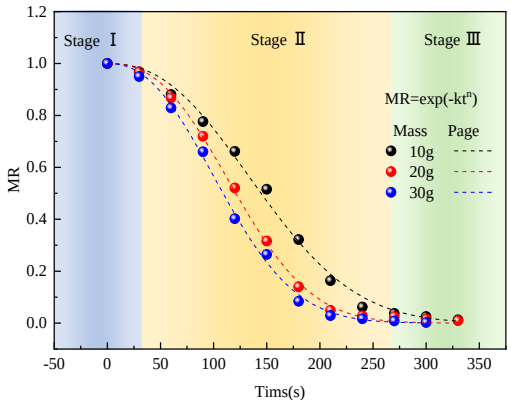

(a)

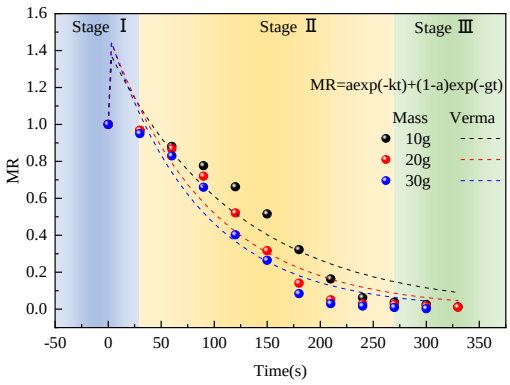

(b)

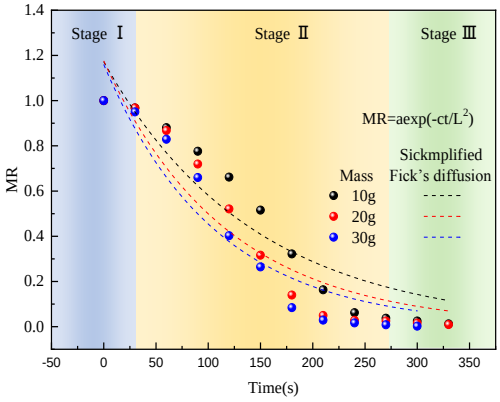

(c)

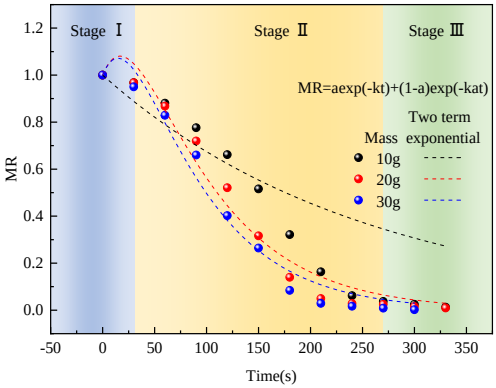

(d)

Fig. 9. Fitting curves of different drying kinetic models and drying experimental data of APV under different mass resulting from (a) Page; (b) Verma; (c) Simplified Fick's diffusion; (d) Two-term exponential.

Table 6 Fitting data of drying kinetics model of APV with different as received sample mass.

Model	Mass/g	Params	R^2	RSS	F-value
Page	10g	k=5.5127*10^{-6}, n=2.36041	0.99549	0.00699	2967.61107
	20g	k=4.9427*10^{-6}, n=2.47141	0.99883	0.00191	9408.3118
	30g	k=1.3525*10^{-5}, n=2.31204	0.99806	0.00284	5170.77103
Verma	10g	k=0.00833, a=1.40707, g=24645.1035	0.9191	0.11275	107.53139
	20g	k=0.01056, a=1.49244, g=24645.1035	0.94156	0.08574	123.03775
	30g	k=0.01173, a=1.4985, g=20103.47527	0.94746	0.06838	124.68051
Simplified Fick's diffusion	10g	c= 0.0293, a= 1.17244, L=2.04297	0.9191	0.11275	107.53139
	20g	c= 0.03422, a= 1.17594, L= 1.99864	0.94156	0.08574	123.03775
	30g	c= 0.03722, a= 1.1602, L= 1.99229	0.88941	0.14392	57.83823
Two term exponential	10g	a= 0.99756, k= 0.00394	0.69287	0.4756	38.67178
	20g	a= 2.34999, k= 0.0133	0.97446	0.04163	427.62615
	30g	a= 2.32613, k= 0.01458	0.97678	0.03399	427.76456

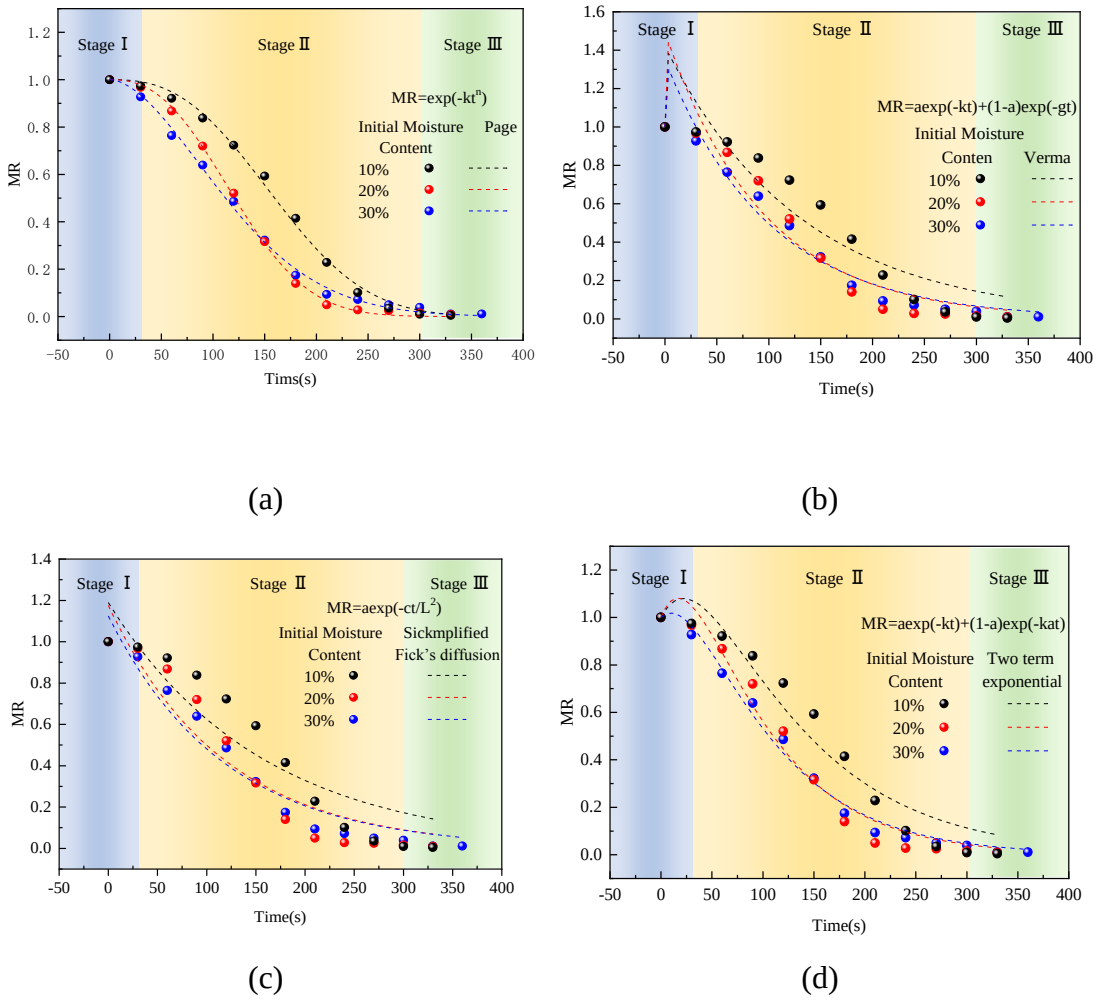

Fig. 10. Fitting curves of drying experimental data of APV with different drying kinetic models and different initial moisture content resulting from: (a) Page; (b) Verma; (c) Simplified Fick's diffusion; (d) Two-term exponential.

Table 7 Fitting data of drying kinetics model of APV with different initial moisture content.

Model	Initial moisture content /%	Params	R^2	RSS	F-value
Page	10%	$k= 1.1236*10^{-6}$ n= 2.62819	0.99637	0.00582	3956.4067
	20%	$k= 4.9427*10^{-6}$	0.99883	0.00191	9408.3118

		n= 2.47141			
	30%	k= $1.6255*10^{-4}$ n= 1.77103	0.99716	0.00422	4222.13622
Verma	10%	a= 1.41976, k=0.00762, g= 26493.1175	0.89104	0.15731	84.93142
	20%	a= 1.49244, k=0.01056, g= 24645.1035	0.94156	0.08574	123.03775
	30%	a= 1.34789, k= 0.01, g= 15490.7992	0.97366	0.03559	300.35641
Simplified Fick's diffusion	10%	a= 1.18953,c=0.01173, L= 1.35054	0.83732	0.23487	55.89457
	20%	a= 1.17594,c=0.03422, L= 1.99864	0.88519	0.16846	61.14844
	30%	a= 1.12499,c=0.04648, L= 2.3391	0.94266	0.07748	136.18068
Two term exponential	10%	a= 2.34702,k= 0.01008	0.94849	0.08263	274.00365
	20%	a= 2.34999, k= 0.0133	0.97446	0.04163	427.62615
	30%	a= 2.15029, k=0.01263	0.99046	0.01418	1251.87451

Besides, the normal distribution diagram and residual scatter diagram are usually used as reference verifications for the evaluations of the fitting curves and experimental data. Thus, the method of mathematical statistics analysis was used to analyse the residual of different fitting models with normal probability distribution maps as shown in Fig. 11, indicating that the page model is closer to a straight line compared to the normal probability distribution of the other three model fitting results, rendering to the experimental data can be well fitted with Page model. The

standard residual scatter map of the Page model is shown in Fig. 12, suggesting that the residual distribution of the Page model and experimental data is random, which indicates that the experimental results are correct.

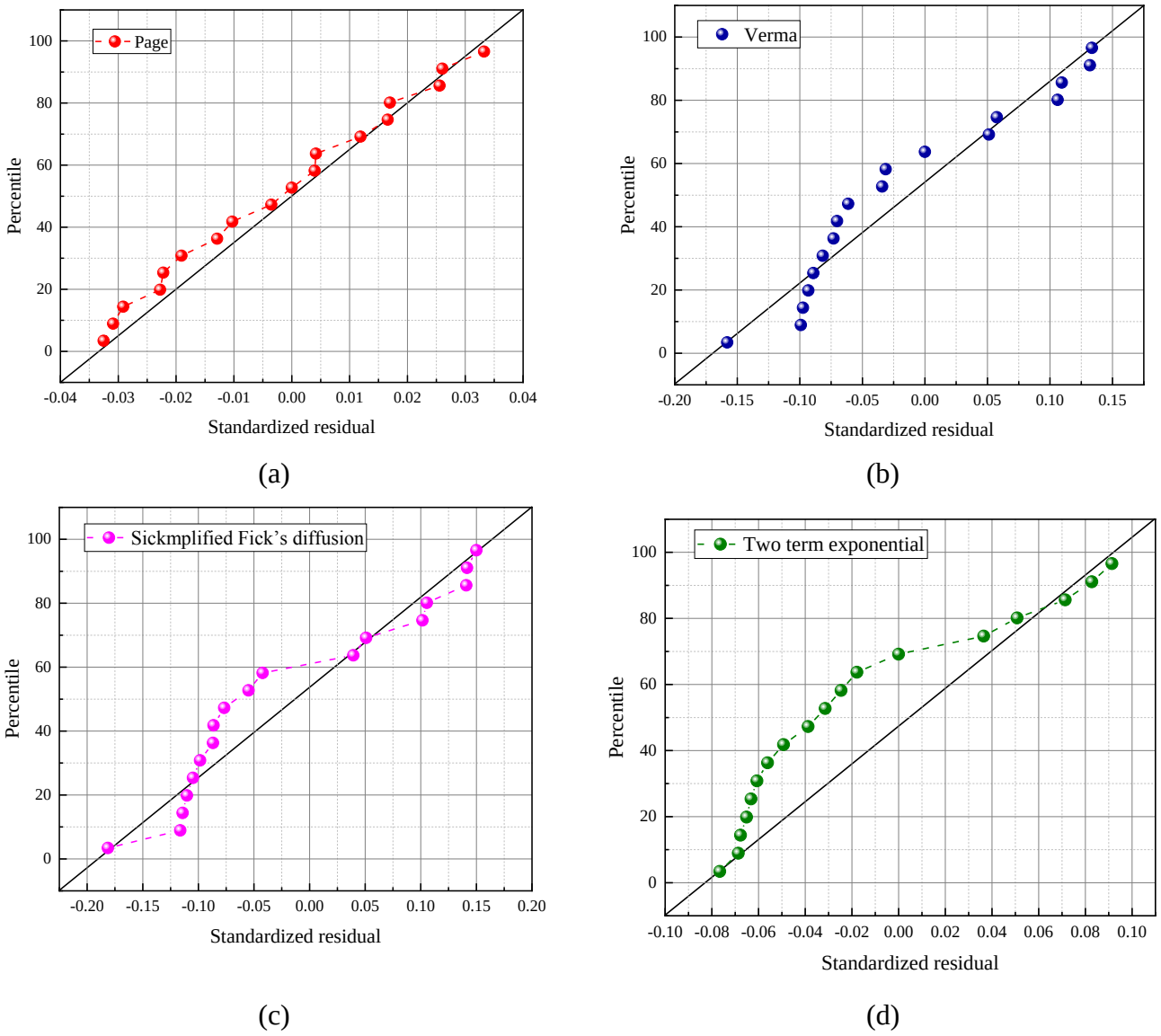

Fig. 11. Normal probability diagram and data fitting of drying kinetic model resulting from (a) Page; (b) Verma; (c) Simplified Fick's diffusion; (d) Two-term exponential.

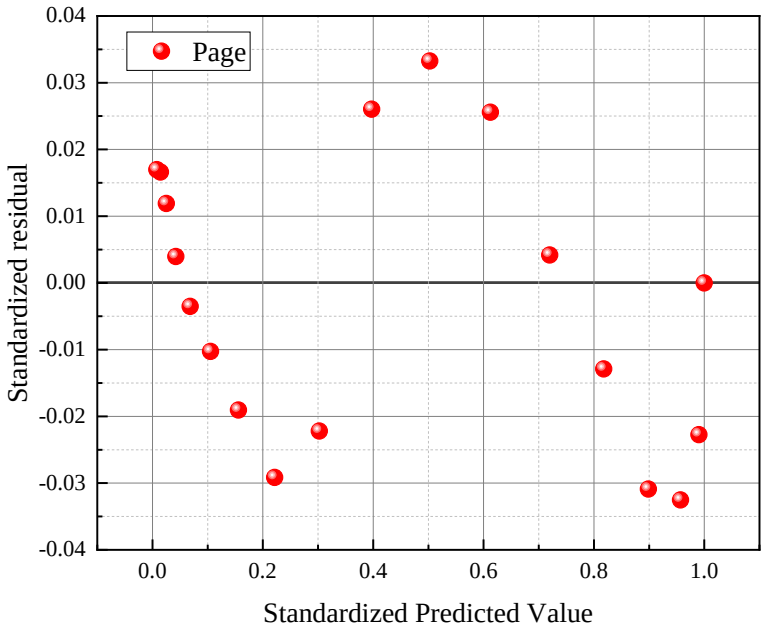

Fig. 12. Residual scatter diagram of Page model.

3.5.2 Dynamic analysis of hot air drying

To find the drying kinetic model of the hot air drying process of APV. The experimental data were fitted with the same dynamic models as mentioned in the last section. The fitting results are given in Table 8. By comparing R^2, RSS, F-value, and other parameters, it is found that the model with the highest matching degree with hot air drying process is still the Page model, and the fitting figure is shown in Fig. 13.

Table 8 The fitting parameters of hot air drying kinetics.

Model	Params	R^2	RSS	F-value
Page	k= 1.67002*10^{-4} n= 1.7678	0.99973	4.10499*10-4	43479.93127
Verma	a= 1.37055 k= 0.01023 g= 17065.47219	0.97862	0.02939	364.72133
Simplified Fick's	a= 1.13133	0.94464	0.07613	138.78004

diffusion	c= 0.04649 l= 2.32406			
Two term exponential	a= 2.17469 k= 0.01287	0.99416	0.00883	2015.63909

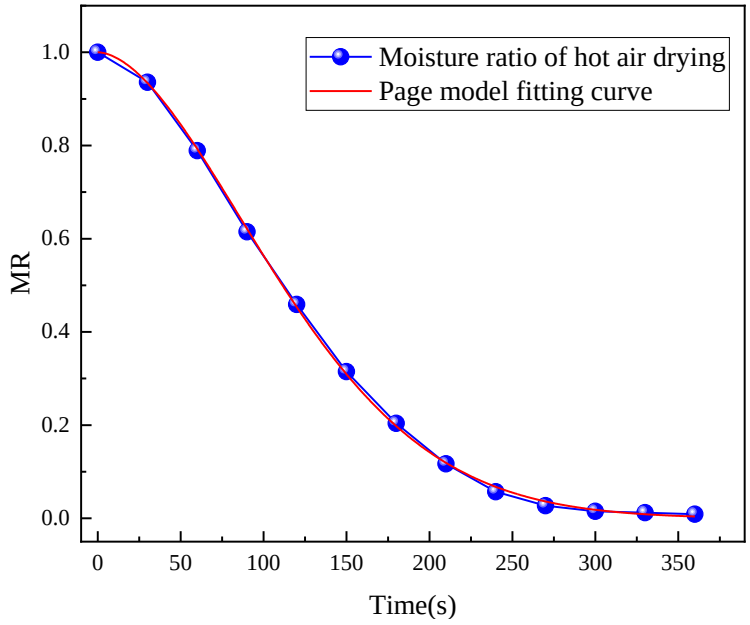

Fig. 13. Hot air drying moisture ratio and page model fitting curve.

4. Conclusions

In this paper, the effects of different microwave power, mass, and initial moisture content on the characteristics of microwave drying of APV powder were studied. Additionally, to understand the kinetics during microwave drying, four kinetic models, namely Page model, Verma model, Simplified Fick's dispersion model, and Two-term experimental model were employed for experimental data fitting. The conclusions are as follows:

(1) Microwave power has a significant impact on the drying performance of APV

powder. The dehydration effect has a positive relation with microwave power. The material will absorb more microwave energy and convert it into heat energy with the increase in the microwave heating power, thus accelerating the internal heat and mass transfer. Maximum drying rate of APV with microwave powers of 280W, 350W, 560W and 700W were $0.000852s^{-1}$, $0.00106s^{-1}$, $0.00134s^{-1}$ and $0.00134s^{-1}$, respectively. The corresponding time for reaching these peak drying rates were 240s, 150s, 120s, and 120s, respectively.

(2) The effect of material quality on the drying performance of APV has obvious regularity, and the quality of the as-received powder sample has a positive relationship with the drying efficiency. The maximum drying rate of APV with sample masses of 10g, 20g, and 30g were $0.00117\ s^{-1}$, 0.00134^{-1}, and $0.00142s^{-1}$, respectively. The corresponding time for reaching these peak drying rates were 180s, 120s, and 90s, respectively. It should be noticed that this conclusion only fits sample quality in the studied range. For samples with large quantities, the heating efficiency may show a negative relation with sample mass depending on the penetrate thickness of the microwave on the sample, which needs further investigation.

(3) The effect of initial moisture content on the drying performance of APV was also significant. The drying performance of the as-received sample at an initial moisture content of 30% was better than that at an initial moisture content of 10% or 20%, which was benefiting from the positive relation between moisture content and microwave energy absorption efficiency, and was contrary to the common sense received from conventional heating. The maximum drying rate of APV powder with

initial moisture contents of 10%, 20% and 30% were 0.000382s^{-1}, 0.00134s^{-1}, and 0.00182s^{-1}, respectively. The corresponding time for reaching these peak drying rates were 120s, 120s, and 180s, respectively.

(4) Additionally, the above experimental data were fitting with four classical drying kinetic models to understand the mechanism of microwave drying. The results indicated that the Page model was robust in describing the kinetics of microwave drying and hot air drying of APV with a decent fitting degree and F-Value, and the R^2 value for the fitting curve was close to 1.

Declaration of competing interests

The authors declare that they have no known competing financial interests or personal relationships that could have appeared to influence the work reported in this paper.

Acknowledgements

Financial supports from the National Natural Science Foundation of China (No: U1802255, 51404114 and 51504110), the National Key R&D Program of China (2018YFC1900500), the Key Projects in the National Science & Technology Pillar Program during the Twelfth Five-year Plan Period (No. 2015BAB17B00), and Innovative Research Team (in Science and Technology) in University of Yunnan Province were sincerely acknowledged.

References

[1] H. Wan, B. Xu, L. Li, B. Yang, D. Li, Y. Dai, A novel method of fabricating Al-V interme-tallic alloy through electrode heating, Metals, 9 (5) (2019) 558.

[2] D. Casari, T. Ludwing, M. Merlin, L. Arnberg, G. Garagnani, The effect of Ni and V trace elements on the mechanical properties of A356 aluminium foundry alloy in as-cast and T6 heat treated conditions, Materials Science and Engineering: A, 610 (2014) 414-426.

[3] G. Li, Y. Qiu, Y. Hou, H. Li, L. Zhou, H. Deng, Y. Zhang, Synthesis of V_2O_5 hierarchical structures for long cycle-life lithium-ion storage, Journal of Materials Chemistry A, 3 (3) (2015) 1103-1109.

[4] A. Cao, J. Hu, H. Liang, L. Wan, Self-assembled vanadium pentoxide (V_2O_5) hollow microspheres from nanorods and their application in Lithium-ion batteries, Angewandte Chemie International Edition, 117 (28) (2005) 4465-4469.

[5] Y. Lu, Y. Wen, F. Huang, T. Zhu, S. Sun, B. Benicewicz, K. Huang, Rational design and demonstration of a high-performance flexible Zn/V_2O_5 battery with thin-film electrodes and para-polybenzimidazole electrolyte membrane, Energy Storage Materials, 27 (2020) 418-425.

[6] M. Pawar, M. Sutar, K. Maddani, S. Kandalkar, Improvement in electrochemical performance of spray deposited V_2O_5 thin film lectrode by anodization, Materials Today: Proceedings, 4 (2) (2017) 3549-3556.

[7] R. Zhang, T. Zhao, H. Jiang, M. Wu, L. Zeng, V_2O_5-NiO composite nanowires: A novel and highly efficient carbon-free electrode for non-aqueous Li-air batteries operated in ambient air, Journal of Power Sources, 409 (2019) 76-85.

[8] X. Ren, D. Ai, R. Lv, F. Kang, Z. Huang, Facile preparation of V_2O_5/PEDOT core-shell nanobelts with excellent lithium storage performance, Electrochimica Acta,

336 (2020) 135723.

[9] A. Pan, H. Wu, L. Zhang, X. Lou, Uniform V_2O_5 nanosheet-assembled hollow microflowers with excellent lithium storage properties, Energy & Environmental Science, 6 (5) (2013) 1476-1479.

[10] J. Shen, S. Liu, Z. He, L. Shi, Influence of antimony ions in negative electrolyte on the electrochemical performance of vanadium redox flow batteries, Electrochimica Acta, 151 (2015) 297-305.

[11] X. Guo, C. Zhang, Q. Tian, D. Yu, Liquid metals dealloying as a general approach for the selective extraction of metals and the fabrication of nanoporous metals: A review, Materials Today Communications, 26 (2021) 102007.

[12] P. Chithaiah, G. Vijaya Kumar, G. Nagabhushana, G. Nagaraju, G. Chandrappa, Synthesis of single crystalline $(NH_4)_2V_6O_{16}\cdot 1.5H_2O$ nest-like structures, Physica E: Low-dimensional Systems and Nanostructures, 59 (2014) 218-222.

[13] L. Wang, D. Xu, L. Wang, X. Zhang, Facile and low-cost synthesis of large-area pure V_2O_5 nanosheets for high-capacity and high-rate lithium storage over a wide temperature range, ChemPlusChem, 77 (2) (2012) 124-128.

[14] Z. Wu, Study on vanadium solution dissolved sediment in wastewater from vanadium precipitation, International Conference on Chemical Engineering, 581 (2012) 172-175.

[15] B. Makuza, Q. Tian, X. Guo, K. Chattopadhyay, D. Yu, Pyrometallurgical options for recycling spent lithium-ion batteries: A comprehensive review, Journal of Power Sources, 491 (2021) 229622.

[16] E. Kostas, D. Beneroso, J. Robinson, The application of microwave heating in bioenergy: A review on the microwave pre-treatment and upgrading technologies for biomass, Renewable & Sustainable Energy Reviews, 77 (2017) 12-27.

[17] J. Ford, D. Pei, High temperature chemical processing via microwave absorption, Microwave Power, 2 (2) (1967) 61-64.

[18] K. Haque, Microwave energy for mineral treatment processes—a brief review, International journal of mineral processing, 57 (1) (1999) 1-24.

[19] R. Mishra, A. Sharma, Microwave-material interaction phenomena: heating mechanisms, challenges and opportunities in material processing, Composites Part A: Applied Science and Manufacturing, 81 (2016) 78-97.

[20] M. Araszkiewicz, A. Koziol, A. Lupinska, M. Lupinski, IR technique for studies of microwave assisted drying, Drying Technology, 25 (4) (2007) 569-574.

[21] J. Zhu, J. Liu, J. Wu, J. Cheng, J. Zhou, K. Cen, Thin-layer drying characteristics and modeling of Ximeng lignite under microwave irradiation, Fuel Processing Technology, 130 (2015) 62-70.

[22] Z. Ma, Y. Liu, J. Zhou, M. Liu, Z. Liu, Recovery of vanadium and molybdenum from spent petrochemical catalyst by microwave-assisted leaching, International Journal of Minerals, Metallurgy and Materials, 26 (1) (2019) 33.

[23] J. Liu, J. Zhu, J. Cheng, J. Zhou, K. Cen, Pore structure and fractal analysis of Ximeng lignite under microwave irradiation, Fuel. 146 (2015) 41-50.

[24] Y. Li, Y. Lei, L. Zhang, J. Peng, C. Li, Microwave drying characteristics and kinetics of ilmenite, Transactions of Nonferrous Metals Society of China, 21 (1) (2011) 202-207.

[25] A. Idris, K. Khalid, W. Omar, Drying of silica sludge using microwave heating, Applied Thermal Engineering, 24 (5-6) (2004) 905-918.

[26] Y. Ling, Q. Li, H. Zheng, M. Omran, L. Gao, J. Chen, G. Chen, Optimisation on the stability of CaO-doped partially stabilised zirconia by microwave heating, Ceramics International, 47 (6) (2021) 8067-8074.

[27] J. Wang, T. Jiang, Y. Liu, X. Xue, Influence of microwave treatment on grinding and dissociation characteristics of vanadium titano-magnetite, International Journal of Minerals, Metallurgy and Materials, 26 (2) (2019) 160.

[28] K. Li, J. Chen, J. Peng, R. Ruan, M. Omran, G. Chen, Dielectric properties and thermal behaviour of electrolytic manganese anode mud in microwave field, Journal of Hazardous Materials, 384 (2020) 121227.

[29] K. Li, J. Chen, J. Peng, R. Ruan, C. Srinivasakannan, G. Chen, Pilot-scale study on enhanced carbothermal reduction of low-grade pyrolusite using microwave heating, Powder Technology, 360 (2020) 846-854.

[30] N. Dandapat, S. Ghosh, Development of non-shrinkable ceramic composites for use in high-power microwave tubes, International Journal of Minerals, Metallurgy and Materials, 26 (4) (2019) 516.

[31] X. Wang, H. Lin, Y. Dong, G. Li, Bioleaching of vanadium from barren stone coal and its effect on the transition of vanadium speciation and mineral phase, International Journal of Minerals, Metallurgy and Materials, 25 (3) (2018) 253.

[32] Y. Ling, Q. Li, H. Zheng, M. Omran, L. Gao, J. Chen, G. Chen, Optimisation on the stability of CaO-doped partially stabilised zirconia by microwave heating, Ceramics International, 47 (6) (2020) 8067-8074.

[33] K. Li, Q. Jiang, G. Chen, L. Gao, J. Peng, Q. Chen, S. Koppala, M. Omran, J. Chen, Kinetics characteristics and microwave reduction behaviour of walnut shell-pyrolusite blends, Bioresource Technology, 319 (2021) 124172.

[34] G. Chen, Q. Li, Y. Ling, H. Zheng, J. Chen, Q. Jiang, K. Li, J. Peng, M. Omran, L. Gao, Phase stability and microstructure morphology of microwave-sintered magnesia-partially stabilised zirconia, Ceramics International, 47 (3) 2020 4076-4082.

[35] K. Li, J. Chen, J. Peng, S. Koppala, M. Omran, G. Chen, One-step preparation of

CaO-doped partially stabilised zirconia from fused zirconia, Ceramics International, 46 (5) (2020) 6484-6490.

[36] D. Chen, D. Li, Y. Zhang, Z. Kang, Preparation of magnesium ferrite nanoparticles by ultrasonic wave-assisted aqueous solution ball milling, Ultrason. Sonochem, 20 (6) (2013) 1337-1340.

[37] B. Chen, D. Chen, Z. Kang, Y. Zhang, Preparation and microwave absorption proper-ties of Ni-Co nanoferrites, Journal of Alloys and Compounds, 618 (2015) 222-226.

[38] H. Hacifazlioglu, Comparison of efficiencies of microwave and conventional electric ovens in the drying of slime-coal agglomerates, International Journal of Coal Preparation and Utilization, 37 (4) (2016) 169-178.

[39] K. Li, J. Chen, G. Chen, J. Peng, R. Ruan, C. Srinivasakannan, Microwave dielectric properties and thermochemical characteristics of the mixtures of walnut shell and manganese ore, Bioresource Technology, 286 (2019) 121381.

[40] S. Guo, G. Chen, J. Peng, J. Chen, D. Li, Microwave assisted grinding of ilmenite ore, Transactions of Nonferrous Metals Society of China, 21 (9) (2011) 2122-2126.

[41] C. Ai, P. Sun, A. Wu, X. Chen, C. Liu, Accelerating leaching of copper ore with surfactant and the analysis of reaction kinetics, International Journal of Minerals, Metallurgy and Materials, 26 (3) (2019) 274.

[42] B. Fu, M. Chen, Q. Li, Heat transfer characteristics and drying kinetics of hematite thin layer during hot air convection, Thermochimica Acta, 682 (2019) 178405.

[43] X. Zeng, F. Wang, M. Adamu, L. Zhang, Z. Han, G. Xu, High-temperature drying behaviour and kinetics of lignite tested by the micro fluidization analytical method, Fuel, 253 (2019) 180-188.

[44] Y. Xu, X. Qin, G. Zhang, Y. Zhang, An experimental investigation on the drying characteristics and kinetics of Baorixile lignite in a fixed bed, Feul, 253 (2019) 1317-1324.

[45] X. Li, H. Song, Q. Wang, C. Meesri, T. Wall, J. Yu, Experimental study on drying and moisture re-adsorption kinetics of an Indonesian low rank coal, Journal of Environmental Sciences, 21 (2009) S127-S130.

[46] J. Du, L. Gao, Y. Yang, S. Guo, J. Chen, M. Omran, G. Chen, Modeling and kinetics study of microwave heat drying of low grade manganese ore, Advanced Powder Technology, 37 (7) (2020) 2901-2911.

[47] A. Tahmasebi, J. Yu, Y. Han, H. Zhao, S. Bhattacharya, A kinetic study of microwave and fluidized-bed drying of a Chinese lignite, Chemical Engineering Research & Design, 92 (1) (2014) 54-65.

[48] Q. Zhang, J. Litchfield, An optimization of intermittent corn drying in a laboratory scale thin layer dryer, Drying Technology, (9) (1991) 383–395.

[49] G. Page, Factors Influencing the Maximum Rates of Air Drying Shelled Corn in Thin Layers, Department of Mechanical Engineering, Purdue University, West Lafayette, 1949.

[50] Y. Sharaf-Eldeen, J. Blaisdell, M. Hamdy, A model for ear-corn drying, ASAE, 23 (1980) 1261–1265.

[51] L. Verma, R. Bucklin, J. Endan, F. Written, Effects of drying air parameter on rice drying models, ASAE, 28 (1985) 296–301.

[52] L. Diamante, P. Munro, Mathematical modelling of hot air drying of sweet potato slices, International Journal of Food Science & Technology, 26 (1991) 99–109.

- Microwave drying technology for ammonium polyvanadate (APV) was studied.
- The kinetics of microwave drying was studied with experimental data fitting.
- Page model was robust on describing the microwave drying process of APV.

Graphical Abstract (for review)

Click here to access/download;Graphical Abstract (for review);graphic abstract.docx

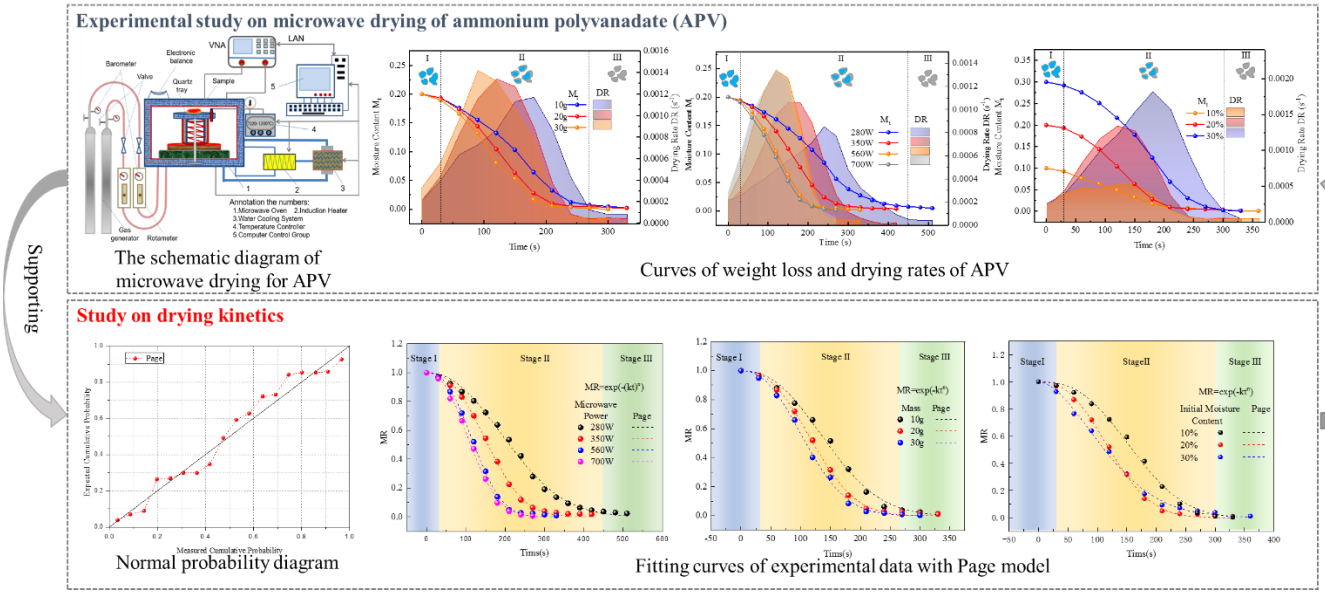

Conflict of interest statement

We declare that we have no financial and personal relationships with other people or organizations that can inappropriately influence our work, there is no professional or other personal interest of any nature or kind in any product, service and/or company that could be construed as influencing the position presented in, or the review of, the manuscript entitled, "*Research of Microwave Drying Technology in the Procedure of Preparation of V_2O_5 from Ammonium Polyvanadate (APV)*" by Hewen Zheng, Qiannan Li, Yeqing Ling, Mamdouh Omran, Lei Gao, Jin Chen and Guo Chen.